Nanoindentation and Raman studies of phase-separated Ag-As-S glasses

K. S. Andrikopoulos, J. Arvanitidis, V. Dracopoulos, D. Christofilos, T. Wagner et al.

Related Articles

One-particle correlation function in evanescent wave dynamic light scattering
J. Chem. Phys. 136, 204704 (2012)

Near-field artifacts in tip-enhanced Raman spectroscopy
Appl. Phys. Lett. 100, 213111 (2012)

Compositional effect of WO3, MoO3, and P2O5 on Raman spectroscopy of tellurite glass for broadband and high gain Raman amplifier
J. Appl. Phys. 111, 103511 (2012)

Calculation of the lattice dynamics and Raman spectra of copper zinc tin chalcogenides and comparison to experiments
J. Appl. Phys. 111, 083707 (2012)

Low-damping spin-wave propagation in a micro-structured Co2Mn0.6Fe0.4Si Heusler waveguide
Appl. Phys. Lett. 100, 112402 (2012)

Additional information on Appl. Phys. Lett.

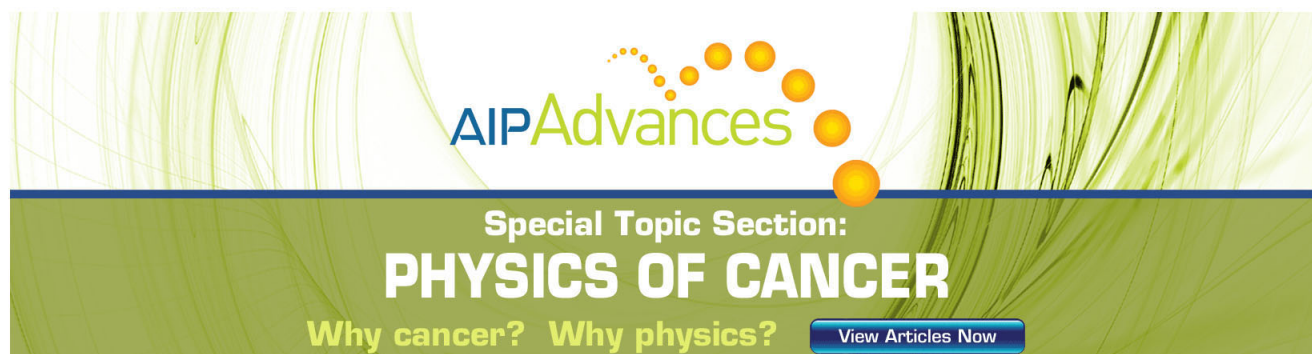Journal Homepage: http://apl.aip.org/

Journal Information: http://apl.aip.org/about/about_the_journal

Top downloads: http://apl.aip.org/features/most_downloaded

Information for Authors: http://apl.aip.org/authors

Nanoindentation and Raman studies of phase-separated Ag-As-S glasses

K. S. Andrikopoulos,[1,2,a)] J. Arvanitidis,[1] V. Dracopoulos,[2] D. Christofilos,[3] T. Wagner,[4] and S. N. Yannopoulos[2,5]

[1]Department of Applied Sciences, Technological Educational Institute of Thessaloniki, 57400 Sindos, Greece
[2]Foundation for Research and Technology Hellas (FORTH/ICE-HT), P.O. Box 1414, GR-26 504 Patras, Greece
[3]Physics Division, School of Technology, Aristotle University of Thessaloniki, GR-54124 Thessaloniki, Greece
[4]Department of Inorganic Chemistry, Faculty of Chemical-Technology, University of Pardubice, Legiońs sq. 565, 53210, Pardubice, Czech Republic
[5]Department of Materials Science, University of Patras, GR-26 504 Patras, Greece

Nanoindentation is used to study the mechanical properties at the nanoscale of the ternary $Ag_x(As_{0.33}S_{0.67})_{100-x}$ glassy system for $0 \leq x \leq 25$. Direct evidence for phase separation of a Ag-poor and a Ag-rich phase in the composition range $2 \leq x \leq 20$ is provided. The volume of the Ag-rich phase increases with x and percolates at $x \approx 7$. The mechanical properties of the Ag-rich phase are comparable to those of the $x = 25$ glass, while those of the Ag-poor phase are closer to (however, quite different from) the ones of the base glass AsS_2. The structure of both phases at short and medium range order is investigated by micro-Raman spectroscopy and is correlated to their mechanical properties. © 2011 American Institute of Physics. [doi:10.1063/1.3651494]

Non-crystalline chalcogenides, either bulk or thin films, are promising materials for a wide range of electronics and photonics applications.[1,2] Their optical bandgap falls within the visible and the near-IR range and can be simply tailored by fine tuning the alloy's composition; this semiconducting nature combined with a high photosensitivity constitute the hallmark of chalcogenides and lie at the origin of many of their applications. In most cases, phase separation—a common effect in melt-quenched glasses—is an undesirable effect for applications in optics. However, its role has proved quite interesting when electrical properties are considered. Especially, near the percolation threshold where the originally fragmented phase becomes continuous, the electrical conductivity increases abruptly by several orders of magnitude.[3]

With respect to the host glass of this investigation, binary arsenic sulfides, As_xS_{100-x} are amongst the most thoroughly studied systems that can easily form macroscopically homogeneous glasses in the range $0 \leq x \leq 42$.[4] However, these glasses cannot be considered strictly homogenous at the nanoscale where various local environments such as S_n-chains, S_8-rings, and "$AsS_{3/2}$" pyramidal units co-exist, whose concentration depend on x.[5]

Silver-containing chalcogenides have recently gained increased interest as emerging solutions in resistive-switching random access memories employing the configuration of a metal-insulator-metal memory cell.[6] The switching mechanism is actually based on the polarity dependent electrochemical deposition and removal of metal in a thin solid state electrolyte film, which is usually a chalcogenide glass. Phase separation creates droplets of a silver-rich conductive phase within the electrolyte matrix structure, and hence the switching mechanism can become much faster because a much shorter percolative pathway needs to be built between the droplets of the conductive phase.[7] A detailed characterization of the phases involved in such micro-phase separated systems is needed for illuminating various aspects of the switching mechanisms which still remain unclear.

In this letter, we present a nanoindentation mapping study of the mechanical properties of selected glasses from the phase-separated system $Ag_x(As_{0.33}S_{0.67})_{100-x}$ combined with micro-Raman structural characterization of the two phases at molecular level. Mapping the mechanical properties at the nanoscale employing nanoindentation testing provides a direct evaluation of the mechanical properties of these systems that cannot be explored by other experimental techniques.

Glasses were prepared from proper mixing of high purity elements at high temperature and melt-quenching. The ingots were cut into rectangular slabs which were then polished to optical quality. Details related to sample preparation can be found elsewhere.[8] Nanoindentation measurements were performed by means of a Hysitron Tribolab instrument equipped with a Berkovich-type tip. A trapezoidal loading function was applied to all glasses.[9] The mechanical properties of the two end members of the glassy system of interest (i.e., the AsS_2, $x = 0$ and the $AgAsS_2$, $x = 25$) were thoroughly studied since these samples served as reference for the evaluation of the mechanical properties of the phase separated glasses. The reduced elastic modulus (E_r) and nanohardness (H) were determined from the experimental unload-displacement curves using the Oliver and Pharr model[10] and their mean values were calculated after statistical analysis of several measurements. Raman spectra, with a spectral resolution of $\sim 2\,cm^{-1}$, were excited with the 780 nm laser line of a Ti-Sapphire laser and recorded using a triple monochromator DILOR XY instrument equipped with a liquid-nitrogen cooled CCD. A $100\times$ objective was employed, providing a spot size of $\sim 1\,\mu m$ on the sample.

Optical micro-photographs of representative samples from the ternary system $Ag_x(As_{0.33}S_{0.67})_{100-x}$ are illustrated in Fig. 1. Due to the high quality of the sample's surface, it was possible to obtain evidence of single glass phase for samples with $x = 0$, 22, 24, and 25. At low Ag concentration, $x < 8$, the
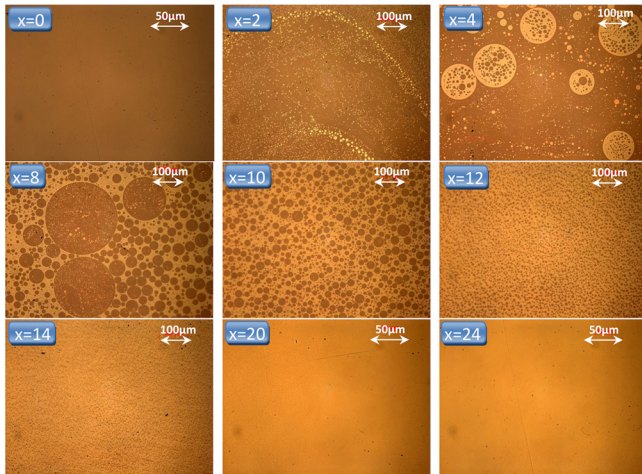
a)Electronic mail: kandriko@gen.auth.gr.

FIG. 1. (Color online) Optical micro-photographs using $50\times$ and $20\times$ objectives for the $x=0$, 20, 24 and $x=2$, 4, 8, 10, 12, 14 samples, respectively.

TABLE I. Mean values and standard deviations of the elastic modulus and hardness for the samples under investigation obtained from nano-indentation measurements. Hardness obtained from micro-hardness experiments on similar compositions are given in the last column.

Sample's Composition	Nanoindentation measurements		Microhardness measurements[4]
	Modulus (GPa)	Hardness (GPa)	Hardness (GPa)
AsS_2[a]	18.2 ± 0.45	1.56 ± 0.060	1.05
$AgAsS_2$[a]	37.7 ± 0.53	2.27 ± 0.057	1.46
$Ag_8As_{31}S_{61}$[b,c]	28.3 ± 1.97	1.98 ± 0.15	—
$Ag_8As_{31}S_{61}$[b,d]	37.2 ± 3.46	2.33 ± 0.3	—
$Ag_{10}As_{33}S_{57}$[b]	—	—	1.57

[a]Homogeneous sample.
[b]Phase separated sample.
[c]Ag–poor phase.
[d]Ag–rich phase.

glasses exhibit phase separation with the phase A, consisting of distinct spherical droplets, incorporated in the continuous phase B. When the Ag concentration reaches ~ 8 at. % the initially continuous phase B becomes fragmented and phase A percolates in the glass structure. The size, type, and number of the droplets depend on the Ag content. Referring to their size, the largest spheres are observed for the samples with Ag content $x=4$, 8, and 10 (their size spans values from $\sim 1\,\mu m$ to several tens of μm). X-ray microanalysis[8] revealed that phases A and B are the Ag-rich ($AgAsS_2$) and the Ag-poor (AsS_2 with small concentration of Ag) phases, respectively.

Table I contains parameters related to the mechanical properties extracted by the nanoindentation measurements; despite the fact that the absolute values are somewhat different than those obtained from micro-hardness experiments performed on materials with similar compositions[4] (last column of the table), the results appear to be consistent at least qualitatively. Images captured by scanning the samples' surfaces with the indenter (AFM mode) revealed inhomogeneous patterns of the mechanical properties, for the glasses with compositions $2 \leq x \leq 20$, in accordance with the optical images. Figure 2(a) depicts an AFM topography of the $Ag_8(As_{0.33}S_{0.67})_{92}$ sample's surface, where the phase separation is evident.

The reduced elastic modulus and the nano-hardness values of the sample region shown in Fig. 2(a) were acquired by a number of sequential nanoindentations and a subsequent calculation of E_r and H for each measurement. The results obtained for the elastic modulus are presented as a contour map in Fig. 2(b) and are in accordance with the scanned image. Indentations performed in the "dark" area of the A phase (Ag-rich phase) resulted in mechanical properties similar to those of the $AgAsS_2$ glass (Table I); representative load/unload curves can be seen in Fig. 2(c). On the other hand, indentations performed in the B phase (Ag-poor phase) yield significantly lower values for both E_r and H. However, it is interesting to note that these values did not exactly match those of the binary AsS_2 system (base glass), indicating that the B phase probably contains a small amount of Ag. The standard deviations in Table I indicate considerable dispersion in the extracted values for each of these two sets—

compared to the dispersion in the homogeneous AsS_2 and $AgAsS_2$ glasses—that can be attributed to: (i) the fact that within several of the large droplets formed by one phase, there may exist smaller droplets of the second phase and (ii) the complex mechanical response of the sphere boundaries.
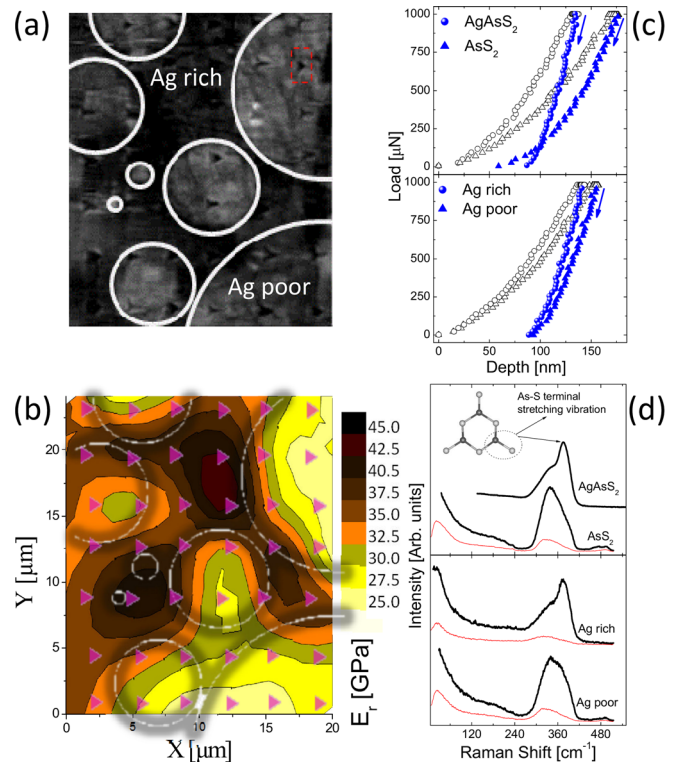

FIG. 2. (Color online) (a) AFM topography of the $Ag_8(As_{0.33}S_{0.67})_{92}$ sample at a $24 \times 20\,\mu m$ region after the accomplishment of 42 sequential indentations (dashed square on the upper right corner encloses a single nanoindentation). White circles have been sketched in order to render the interface between the two phases more visible. (b) Contour map of the elastic modulus. White circles correspond to those in panel (a); Triangles denote approximate positions of single indentations. (c) Single indentations performed on AsS_2 and $AgAsS_2$ samples (top) and on the $x=8$ sample in the Ag-rich and Ag-poor phase (bottom). Open (solid) symbols demonstrate data collected upon load (unload) segment. (d) Raman spectra of the AsS_2 and $AgAsS_2$ glasses (top) as well as the corresponding spectra obtained from the Ag-poor and Ag-rich phase of the $x=8$ sample (bottom). Thick (thin) lines represent VV (VH) spectra. Inset: As_3S_6 structure, the main molecular species existing in the mineral smithite. Dark (light) spheres represent As (S) atoms.

In order to gain more information on the structure of the two phases, micro-Raman spectra were recorded from each one of these. Representative Raman spectra from the two phases for the $x = 8$ glass are shown in the lower panel of Fig. 2(d). Spectra were recorded for two polarization geometries VV and VH where the electric field vectors of the incident and scattered beams are parallel and orthogonal, respectively. In contrast to the constant depolarization ratios measured from macroscopic scattering volumes,[8] frequency dependent depolarization ratios were derived. This result is indicative of a homogeneous glass phase in the scattering volume from which the spectra were collected. The Raman spectra undoubtedly reveal that the structural characteristics of the two phases at molecular level are different. The spectra of the Ag-free (AsS_2) and the $AgAsS_2$ glasses are also illustrated in Fig. 2(d).

The Raman spectrum of the Ag-rich phase exhibits great similarities with that of the $AgAsS_2$ glass [see upper panel in Fig. 2(d) and Ref. 8]. In both spectra, the most intense spectral feature is the band appearing at $\sim 375\,cm^{-1}$. In order to appreciate the difference between the Raman spectra of the AsS_2 and $AgAsS_2$ glasses, we should consider the short and medium range structural order of their corresponding crystals. The structure of the $AgAsS_2$ crystal (either smithite or trechmannite) differs from that of orpiment (As_2S_3), which is a rather good representation of the nearly stoichiometric AsS_2 glass, in that the latter contains layers composed of 6-membered rings (As_6S_{12} groups), while the former ($AgAsS_2$) is a molecular glass where the molecular fragments are 3-membered rings [As_3S_6 groups; see inset of Fig. 2(d) for a planar species building up the smithite allotrope structure]. The units are surrounded by Ag^+ ions interacting with four terminal S atoms, S_t, from four different neighboring As_3S_6 groups. In this context, the existence of As-S_t terminal bonds is indicated by the presence of the peak at $\sim 375\,cm^{-1}$, appearing at higher frequency than the respective stretching vibrations of the pyramidal polyhedra with no terminal S atoms. Besides, it possesses the highest depolarization ratio in the Raman spectrum, as it is expected for a highly polarized vibrational mode of a terminal bond.[11] It is interesting to notice that there is no S excess in the Ag-rich phase and consequently no S-S vibrations are observed in the corresponding Raman spectrum (*vide infra*). The latter is in agreement with a recent structural investigation,[12] which also suggested that the short range order of $AgAsS_2$ glass differs from its crystalline counterpart mostly in that the fourfold coordination of the silver atoms in the glass includes three S atoms and one Ag atom. Given that the Raman bands are dictated by the intramolecular vibrations of the As_3S_6 groups, intermolecular interactions mediated through the weak, ionic Ag-S bonding are not reflected in the Raman spectra, and thus it is precarious to derive arguments about the coordination of Ag atoms from the present study.

The comparison between the Raman spectra of the Ag-free glass with that obtained from the Ag-poor phase reveals also similarities. The main Raman band at $\sim 340\,cm^{-1}$ originates from As-S vibrations in "$AsS_{3/2}$" pyramids where the S atoms are connected either to an As atom of a nearby pyra-

mid (forming corner sharing pyramids) or another S atom (forming either disulfide bonds or longer sulfur segments that interconnect two $AsS_{3/2}$ pyramids). The existence of S-S vibrations belonging to various environments can be justified by the bands appearing in the high frequency region of the spectrum (460–$495\,cm^{-1}$) assigned to: (a) S_n chains, (b) S_8 rings, and (c) disulfide bonds of the type S_2As-S-S-AsS_2.[8] Their intensity appears weaker for the Ag-poor phase compared to that for the case of the Ag-free glass spectrum. The latter designates the comparatively fewer S-S bonds in the Ag-poor phase with respect to the S-S bonds existing in the AsS_2 glass structure, thus suggesting a lower concentration of soft atomic arrangements. This finding accounts for the higher elastic modulus values obtained for the Ag-poor phase in comparison to those of the AsS_2 glass (Table I). Another explanation for the observed differences in the mechanical properties of the two glasses (the one forming the Ag-poor phase and the AsS_2 base glass) may be that the Ag-poor phase contains some amount of Ag which evidently enhances its mechanical properties.

In summary, we have presented a study of the mechanical properties of the ternary $Ag_x(As_{0.33}S_{0.67})_{100-x}$ glassy system at the nanoscale. It was shown that the samples are homogeneous for $x < 2$ and $x > 20$, contrary to the samples of $2 \leq x \leq 20$ composition, which exhibit phase separation with microscopic inhomogeneities characterized by highly symmetric sphere-like domains. The latter was directly observed by the AFM topography as well as by optical microphotographs of the samples' surface; it was also indirectly revealed by the contour map of the modulus obtained after successive nano-indentations. Regardless the sample's composition, one of the phases was found to possess similar mechanical properties to the $x = 25$ sample, while the mechanical properties of the second phase were found to be closer, however not similar, to those of the AsS_2 system. The structure of both phases at short and medium range order was revealed by micro-Raman spectroscopy and was correlated to their mechanical properties.

[1] *Photo-Induced Metastability in Amorphous Semiconductors*, edited by A. V. Kolobov (Wiley-VCH, Weinheim, 2003).
[2] M. Yamane and Y. Asahara, *Glasses for Photonics* (University Press, Cambridge, 2000).
[3] E. A. Kazakova and Z. U. Borisova, Fiz. Khim. Stekla **6**, 124 (1980).
[4] Z. U. Borisova, *Glassy Semiconductors* (Plenum, New York, 1981).
[5] F. Kyriazis and S. N. Yannopoulos, Appl. Phys. Lett. **94**, 101901 (2009).
[6] R. Waser and M. Aono, Nature Mater. **6**, 833 (2007).
[7] M. Kund, G. Beitel, C. U. Pinnow, T. Röhr, J. Schumann, R. Symanczyk, K. D. Ufert, and G. Mueller, in *Proceedings of the International Electron Devices Meeting*, IEDM Tech. Dig. (IEEE, Washington DC, 2005), pp. 754–757.
[8] F. Kyriazis A. Chrissanthopoulos, V. Dracopoulos, M. Krbal, T. Wagner, M. Frumar, and S. N. Yannopoulos, J. Non-Cryst. Solids **355**, 2010 (2009).
[9] The loading-unloading procedure comprised the steps: (i) linear increase of the applied load from 0 up to 1mN within a time interval of 20 s, (ii) 60 s constant load application of 1mN, and (iii) linear total load release within 20 s.
[10] W. C. Oliver and G. M. Pharr, J. Mater. Res. **7**, 1564 (1992).
[11] J. R. Ferraro and K. Nakamoto, *Introductory Raman Spectroscopy* (Academic, Boston, 1994).
[12] V. Kaban, P. Jóvári, T. Wágner, M. Bartoš, M. Frumar, B. Beuneu, W. Hoyer, N. Mattern, and J. Eckert, J. Non-Cryst. Solids **357**, 3430 (2011).